Potentiometric Microsensors

JIŘÍ JANATA

Department of Materials Science and Engineering, University of Utah, Salt Lake City, Utah 84112

Received October 30, 1989 (Revised Manuscript Received February 7, 1990)

Contents

Jiří Janata received his Ph.D. degree in analytical chemistry from Charles University, Prague, Czechoslovakia, in 1965. After 2 years of postdoctoral training at the University of Michigan, he joined Imperial Chemical Industries in England as Head of the analytical development group. In 1976 he became a Professor in the Department of Bioengineering at the University of Utah. In 1987/1988 he spent his sabbatical at the UKAEE Harwell and as a Humboldt Fellow at the UBW Munich. He is currently Professor of Materials Science and Engineering at the University of Utah and a Visiting Professor at the UBW Munich. His research interests include solid-state chemical sensors, electrochemistry, and analytical chemistry.

I. Introduction

According to the electrical parameter that they measure electrochemical sensors can be broadly classified as potentiometric, amperometric, and conductimetric.[1] Classification according to their size is more problematic because size is a relative notion. In order to define the scope of this review, we shall use the method of their fabrication as one classification criterion. Thus, under *potentiometric microsensors* we shall understand electrochemical sensors based on the measurement of potential, which have been fabricated at least in part with the aid of photolithography. This restriction excludes the large and important group of electrochemical sensors–potentiometric microelectrodes used extensively in electrophysiology.[2] The reason for this exclusion is that microelectrodes are a scaled-down version of their macroscopic analogue and their function is similar to regular electrodes. On the other hand, photolithographically prepared potentiometric sensors have certain unique features that set them apart from macroscopic potentiometric sensors although it can be safely stated that each potentiometric microsensor has its macroscopic counterpart. The goal of this review is to underline the most important basic differences between the macro- and micropotentiometric sensors. In the Introduction the factors most important from the point of view of a comparison of macro- and micropotentiometric sensors will be made.

We shall first consider the dimensions of the different types of sensors discussed in this review. Macroscopic potentiometric electrodes[3] are typically of the size of a pencil: ~5 mm in diameter and a few centimeters long. Potentiometric microelectrodes are typically glass capillaries of ~1-μm diameter and again a few centimeters long. Potentiometric microsensors covered in this review are made by more or less conventional techniques used for fabrication of an integrated circuit (IC). Although modern facilities now make ICs with 1-μm lateral resolution, potentiometric microsensors are rarely made with resolution better than 5 μm. Typically, the smallest characteristic dimension of such a sensor is on the order of 10 μm. However, we must understand that this dimension refers to the *active area* of the sensor while the size of the *chip* housing such a sensor may be many times larger (~1000 μm). The important difference between this sensor and a capillary microelectrode is that many active areas (i.e., individual sensors) can be accommodated on a chip of this size together with the associated electronics. This is why they are often called *integrated chemical sensors*. It is this integration of solid-state physics and chemistry that opens some interesting new electrochemistry. The scope of application of IC techniques is further illustrated by fabrication of combined multisensor chip housing both amperometric and potentiometric microsensors[4] and even miniaturized blood gas analyzer fabricated on a silicon wafer.[5]

There is another dimension not yet mentioned and that is the thickness of the individual layers. In this respect IC fabrication techniques are far superior to any manipulation that can be done on macroscopic scale. Thicknesses of deposited layers can be controlled in the range from 0.0001 to ~100 μm. Thus, in the lower limit the IC fabrication approaches molecular dimensions, while in its upper limit it reaches to the macroscopic world. The common part of all chemical sensors is the *selective layer*, which in the case of potentiometric sensors is on the order of 100 μm thick.

It is also important to realize that the signal derived from potentiometric sensors is independent of the size of the active area. This is not so in amperometric

0009-2665/90/0790-0691$09.50/0

sensors in which the most important parameter is the relative area of the two electrodes: The working electrode must be much smaller than the reference electrode. This is an important distinction that sets potentiometric sensors apart from amperometric or conductimetric sensors. Because of this size independence the laws governing the response of potentiometric sensors do not change as we go from macroscopic to microscopic sensors. The price to pay for this advantage is, however, quite substantial: Potentiometric sensors require a stable, well-defined reference electrode because the information about the sample is contained in the *potential difference* between the indicator (potentiometric sensor) and the reference electrode. For this reason we shall also briefly discuss the potentiometric microreference electrode in this review.

Another important difference between the amperometric and the potentiometric sensors lies in the fact that in the former the signal depends on the mass transport whereas in the latter it does not. This means that the convective component (i.e., stirring) of the mass transport to the surface of an amperometric sensor has to be controlled while it is irrelevant in potentiometric sensors.

A potentiometric signal is the result of charge separation. In order to be analytically useful this process must be selective with respect to the species of interest. It takes place in the *chemically selective layer*, which in ionic sensors is called a *ion-selective membrane*. Thus, selective partitioning of ionic species between the sample solution and the ion-selective membrane is the basic process in ion-selective potentiometric sensors. Generation of ionic species by a highly selective enzymatic reaction and their subsequent detection by potentiometric ionic sensors are the basis of potentiometric enzyme sensors. Similarly, formation of ionic species by hydrolysis of gaseous molecules is the mechanism of operation of so-called Severinghaus electrodes. A relatively new principle of potentiometric sensing is based on chemical modulation of electron work function. In that case, the charge separation involves partitioning of electrons between two electronically conducting phases. It is possible to identify matching pairs of macroscopic/microscopic sensors for ions, enzyme substrates, and gases. These are ion-selective electrodes (ISEs) and ion-sensitive field effect transistors (ISFETs), enzyme electrodes and enzymatic field-effect transistors (ENFETs), and the vibrating capacitor (Kelvin probe) and insulated gate field effect transistors (IGFETs). Potentiometric microsensors based on solvolysis of electrically neutral molecules (so-called Severinghaus electrodes) are problematic, but the phenomenon itself is important in operation of ISFETs.

The pivotal role of the field effect transistor (FET) in all three types of microsensors is far more than the reflection of the personal taste of the author. We have to remember that potentiometric measurements are done at zero faradaic current. Therefore, the high-input impedance of the preamplifier is mandatory for a successful measurement. The field effect transistor is an "impedance transformer" because it can amplify a very low power input signal without distortion. In macroscopic potentiometric measurements it is the input stage of the electrometer (i.e., pH meter). On the other hand, in potentiometric microsensors the FET is the integral part of the sensor itself. Field effect transistors are made by the IC fabrication process. It is therefore natural that a review on potentiometric microsensors deals mainly with these devices, specifically with chemically sensitive field effect transistors.

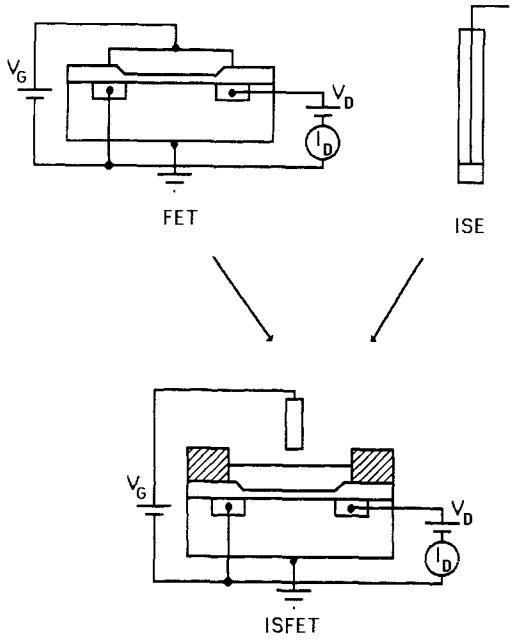

Figure 1. Transition from insulated gate field effect transistor (IGFET) and ion-selective electrode (ISE) to potentiometric microsensor (ISFET).

Let us now recall the dimensional aspects of potentiometric sensors mentioned earlier. In some cases it is possible to transcend from a macro- to a microsensor just by scaling down the macroscopic dimensions (Figure 1). We shall soon see that in reality such procedure is more an exception than a rule and that scaling down involves more than just application of integrated circuit fabrication process.

II. Ion Sensors

The ion-selective membrane can be used in two basic configurations. If the solution is placed on either side of the membrane, such arrangement is called *symmetrical*. It is found in conventional ion-selective electrodes in which the internal electrical contact is provided through the solution in which an internal reference electrode is immersed. In the *nonsymmetrical* arrangement, one side of the membrane is contacted by the sample (usually aqueous) while the other side is contacted by some solid material. In both types the analytically important interface is that between the sample and the ion-selective membrane, which gives rise to the potential difference.

The general tendency to miniaturize chemical sensors and to make them more convenient to use has led to the development of potentiometric sensors with *solid internal contact*. These sensors include macroscopic coated wire electrodes (CWEs), hybrid sensors, and micro ion-sensitive field effect transistors. This contact can be a conductor, semiconductor, or even an insulator. The price to be paid for the convenience of use of these sensors is in the more restrictive design rules that have to be followed in order to obtain sensors with performance characteristics comparable to the conventional

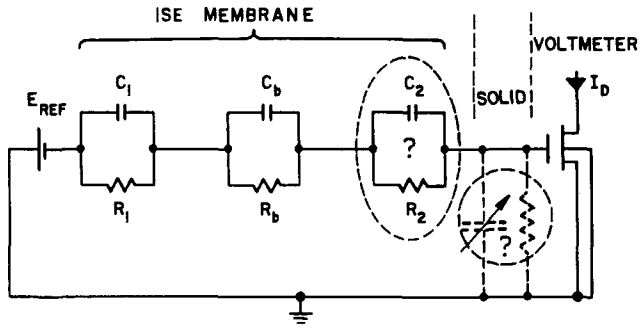

Figure 2. Equivalent electrical circuit of an asymmetrical membrane arrangement. Subscripts b, 1, and 2 refer to the bulk, membrane/sample, and membrane/solid interface.

symmetrical ion-selective electrodes.

The key issue in these sensors is the interface between the ion-selective membrane and the solid phase. The most convenient way to present this problem is in the form of the equivalent electrical circuit in which the resistances and capacitances have their usual electrochemical meaning (Figure 2). Associated with the internal contact is the parasitic capacitance and resistance of the lead wire and of the preamplifier, which must be included in the analysis of the operation of these sensors. In most modern instruments it is an insulated gate field effect transistor which has the input dc resistance in excess of 10^{14} Ω and input capacitance on the order of picofarads.

Let us consider two limiting cases concerning the values of the equivalent resistances in Figure 2. The charge-transfer resistance R_1 is low for a good ion-selective electrode ($i_0 = 10^{-3}$ A cm^{-2}, i.e. $R_{ct} = 25$ Ω cm^2). This means that at least one charged species can transfer relatively easily between the sample and the membrane and establish a stable potential difference. The bulk membrane resistance R_b can be as high as 10^6 Ω cm^2. However, because no net current passes through the membrane, the potential in the bulk of the membrane is uniform; i.e., there is no electric field inside the membrane, and R_b does not have to be considered.

In a conventional symmetrical ISE arrangement, the composition of the internal solution can be always chosen in such a way that the interfacial charge-transfer resistance R_2 is comparable to R_1. Thus, a well-established potential profile exists throughout this structure. On the other hand, if the internal contact resistance R_2 is infinitely high (i.e., no charge transfer between the internal contact and the membrane), the input capacitor together with the interfacial capacitance C_2 and the (variable) parasitic capacitance form a (variable) capacitive divider. In such a case, the voltage appearing at the input capacitor of the electrometer depends not only on the electrostatic potential difference at the membrane/sample interface but also on the undefined parasitic impedance of the connector. Therefore, only *one purely capacitive interface is allowed in a stable potentiometric measurement.* In real situations when the internal contact is a conductor, the interfacial resistance R_2 always has a finite value and as the consequence such an electrode exhibits a slow drift of the signal.

There have been several approaches to the solution of the problem of the internal contact. The most direct way is the interposition of a thin layer of aqueous gel containing a fixed concentration of the salt of the primary ion.[6] This approach, which has been only partially successful, can be seen as the miniaturization of the conventional ISE structure, i.e. return to the symmetrical arrangement for the ion-selective membrane. The main reason why this approach mostly fails upon miniaturization is the fact that electrically neutral species permeate through the membrane and, driven by their chemical potential gradient, establish their own activities inside the sensor structure according to their chemical potential in each individual phase. Therefore, the water permeating through the membrane reaches its osmotic equilibrium pressure according to the activity of the solutes present in the gel. This can lead not only to the significant change of the internal activity of the primary salt inside the gel but often to catastrophic failure of the whole structure when the increase of the osmotic pressure inside the gel exceeds the limits of the mechanical stability of the membrane. This problem is difficult to avoid because the concentration of neutral solutes in the sample is not known a priori and normally cannot be controlled during the measurement.

Another practical problem pertains to the adhesion of the ion-selective membrane to the solid support. In ISFETs with selective membrane deposited directly over the insulator, the adhesion of the membrane can be enhanced by silanization of the ceramic surface and/or by chemical modification of the membrane.[7] Incorporation of the hydrogel sublayer further weakens the structure because the adhesion at the gel/membrane interface is poor.

The second problem relates to the Severinghaus-type interference, which has been observed under certain conditions in ISFETs with ion-selective membrane deposited directly at the insulator. Because water penetrates through the membrane, it hydrates the membrane/insulator interface. When some electrically neutral chemical species with acid/base properties permeates through the membrane (e.g., acetic acid, ammonia, etc.), it hydrolyzes at this interface and may change its local pH, giving rise to a spurious signal.[8] In other words, the hydrated interface between the ion-selective membrane and the insulator behaves like a miniature internal compartment of a Severinghaus electrode. It has been shown that this problem can be avoided in ISFETs by establishing a pH-independent electrochemical process with as high an exchange current density as possible at this interface.[9] Thus, a thin layer of Ag/AgCl has been used. The exchange of chloride ions establishes the interfacial potential, which is independent of any small changes of pH taking place due to the above interference. At the same time, permeation of Cl^- through the membrane to the interface is excluded at the activities below the Donnan failure limit.

In principle, the interference from electrically neutral species can cause problems in a conventional ISE; however, because of the relatively large volume (e.g., 3–5 mL) of internal solution it does not happen in practice. In summary, a potentiometric microsensor incorporating a small volume of the internal electrolyte solution (or a gel) is an example of the scaling-down process that does not work too well.

However, with an understanding of the nature of this problem it is possible ti design potentiometric micro-

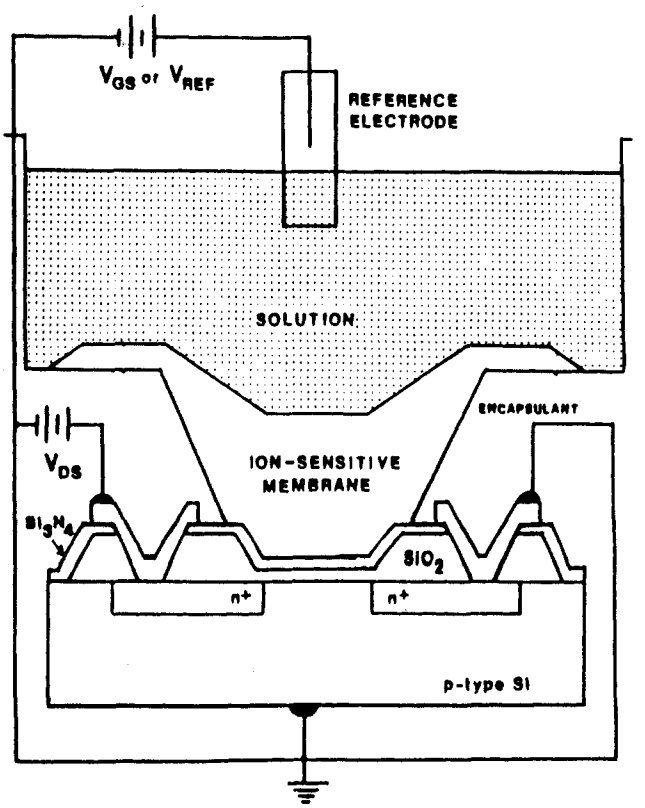

Figure 3. Diagram of an ISFET.

sensors with solid internal contact and to achieve electrochemical performance comparable with a conventional ISE. In summary, the design of the membrane/solid structure has to be done with the understanding of the electrochemical processes at all interfacs. If the final interfacial resistance is high, then problems such as drift will increase with the length of the internal contact, specifically with the magnitude of the parasitic capacitance and resistance. From this, it can be concluded that these problems can be minimized by decreasing the distance between the ion-selective membrane and the amplifier. The problem with the charge-transfer resistance R_2 obviously disappears with the contact itself. Thus, the logical result in miniaturization is the ion-sensitive field effect transistor (Figure 3) in which the ion-selective membrane is placed directly over the gate *insulator* of the FET.

A. Field Effect Transistors

Field effect transistors are part of any modern pH meter. With the introduction of ion-sensitive field effect transistors, they have been brought to the attention of chemists. In order to understand the principles of operation of these new electrochemical devices, it is necessary to include the FET in the overall analysis of the measuring circuit. First, we briefly outline the principles of operation of these semiconductor devices.

1. Semiconductor Field Effect

In an extrinsic semiconductor, containing only one type of dopant, there are equal densities of mobile charges (electrons in n-type and holes in p-type) and ionized dopant atoms (positively charged for n-type and negatively charged for p-type). For simplicity we will restrict this discussion to a p-type extrinsic semiconductor. The condition of electroneutrality applies only in the absence of an external electric field.

If an electric field is applied to the surface of the semiconductor from whatever source, the density of the mobile charge carriers (holes) will be either enhanced or depleted depending on the polarity of the field. If the field enhances the concentration of holes, the surface is said to be accumulated and the semiconductor surface behaves much like a metal in that the excess charge appears at the surface and the electric field does not penetrate it further. If, on the other hand, the field forces the mobile holes away from the surface, a space charge region consisting of the ionized acceptor atoms, which are fixed in the lattice, forms over an appreciable distance into the semiconductor. The thickness of the surface space charge region is a function of the strength of the field at the surface and the semiconductor doping profile, as is the difference between the surface and bulk potentials of the semiconductor. If the surface potential deviates sufficiently far from the bulk potential, the surface will invert; that is, it will contain an excess of mobile electrons. In this case there is an n-type conductive channel on the surface separated from the p-type bulk by a space charge region. A further increase in the normal surface field will not significantly change the surface potential but will only change the density of electrons in the n-type surface layer and, consequently, the electrical conductivity of this layer. Changes in the surface electric field can be determined by measuring the corresponding changes in the thickness of the surface depletion region if the surface is not inverted, or the conductivity of the surface inversion layer if the surface is inverted.

The surface field can be produced in a number of different ways: The semiconductor can be built into a capacitor and an external potential applied, or the field can arise from the electrochemical effects such as partitioning of ions between the sample and the ion-selective membrane. In both cases, changes in the surface electric field change the density of mobile charge carriers in the surface inversion layer. The physical effect that is measured is the change in the electric current carried by the surface inversion layer, the drain current I_D. The devices must be operated under conditions that cause the surface inversion layer to form.

Equation 1 describes the basic current–voltage relationship in the FET operated in so called "nonsaturation" mode ($V_D < V_G - V_T$), where the so-

$$I_D = \frac{\mu_n C_0 W V_D}{L}(V_G - V_T - V_D/2) \qquad (1)$$

called threshold voltage V_T is

$$V_T = V_{FB} + 2\phi_F - Q_B/C_0 \qquad (2)$$

2. Ion-Sensitive Field Effect Transistor

The idea of the first truly integrated chemical sensor, ion-sensitive field effect transistor, was introduced[10,11] in early 1970s. The metal gate of an ordinary IGFET was removed, and the gate insulator was directly exposed to the electrolyte solution. As will be shown later, there is a pH-dependent charge at the insulator/solution interface that contributes to the surface charge. The ISFETs sensitive to different ions can be made by depositing appropriate ion-selective membranes on the FET gate as has been discussed in section II.

A schematic diagram of an ISFET is shown in Figure 3. The metal gate is replaced with a chemically sen-

sitive layer. The electrical path is closed with a reference electrode and the conducting solution. The device is protected by a suitable encapsulant.

The heart of an ISFET is the gate. Equation 1 shows how the gate voltage V_G controls the drain current I_D in the transistor. In an ISFET (Figure 3) the gate has been expanded to include a reference electrode, solution, and the ion-selective membrane. Each interface in this structure contributes its own potential difference, which has to be added to the overall gate voltage.

In the simplest case the solution activity of the ion a^i is related to the interfacial potential at the membrane/solution interface by the Nernst equation

$$\pi = \pi^0 + (RT/z^iF) \ln a^i \quad (3)$$

This potential, together with the reference electrode potential E_{REF}, are added to the externally applied voltage V_G. The resulting voltage has the same meaning and function as that defined for operation of the IGFET (eq 1). Thus, for an ISFET operated in nonsaturation region

$$I_D = \frac{\mu_n C_0 W V_D}{L}(V_G - V_T^* + (RT/z^iF) \ln a^i - E_{REF} - V_D/2) \quad (4)$$

We define V_T^* for an ISFET as

$$V_T^* = V_T - \Delta\phi_{cont} - \pi^0 \quad (5)$$

The inclusion of the term π^0 (but not E_{REF}) in the newly defined threshold voltage is rather arbitrary. The reason for doing so here is that the membrane is physically part of the ISFET, and thus its standard potential should be included in the constant V_T^*. On the other hand, the reference electrode is a completely separate structure, and therefore its potential is kept separate.

Equation 4 relates the activity of the measured ion in the sample to the output of the ISFET in a rather inconvenient way. Mainly for this reason it is preferable to operate the ISFET in so-called "feedback mode". By using, e.g., an operational amplifier in a feedback loop, the current in the ISFET may be held constant. Any change in the potential difference between the solution and the ion-selective membrane due to a change in ionic activity a^i appears as a change in the compensating voltage V_G. Naturally, it is possible to realize the feedback circuit in many different ways either in analog or in digital form, but the basic principle of its function is the same.

pH ISFET. The close integration of the selective layer with the amplifier, as it occurs in the ISFET, offers some unique sensing possibilities. We must remember that a field effect transistor is basically a charge-sensing device. From the very beginning it has been known that an FET with bare gate insulator (SiO_2 or Si_3N_4) exposed to aqueous solution responds to changes of pH. Thus, the surface of the gate insulator can be regarded as a hydrogen ion selective layer. Because pH is such an important parameter to measure, a considerable amount of research has been devoted to the explanation of the mechanism of this response. The slope of this response has been found to vary between 50% of theoretical for SiO_2 to 92% for silicon nitride. Other materials such as Al_2O_3 or Ta_2O_5 and other oxides have been reported to yield nearly theoretical response. It is necessary to pause here and to realize that all these materials are very good bulk insulators and could not be used as pH-sensing materials in a conventional ISE configuration because they would create another capacitor in the circuit. However, in an ISFET these materials *are* the part of the *one capacitor*, the input gate capacitor, and their use is possible. Thus, the usage of these materials for chemical sensing is predictated by the miniaturization process.

It is quite adequate to accept the fact that the pH-dependent charge resides somewhere at the insulator "surface" and that the corresponding image charge in the transistor channel affects the transconductance. The argument about the location of the pH-dependent charge has revolved around the meaning of the term "surface", i.e. around the distinction betwen the polarized and nonpolarized interface. One school of thought has been that the charge is located in one plane at which the charge is generated by the deprotonation/protonation of the surface-bound sites and that the interface behaves as a capacitor. It is tacitly assumed that *no ions* can cross this plane. This is the basis of so-called "site-binding theory" (SBT).[12] In this theory, which has been adopted by some authors for explanation of the pH response of ISFET,[13] it is assumed that there are ionizable binding sites present at the surface of the insulator that determine the distribution of the compensating charge in the adjacent layer of solution. This distribution is the result of the combination of interplay between the thermal forces and electrostatic forces originating in the fixed pH-dependent charge at the surface and is governed by the Poisson–Boltzmann distribution. It should be noted that in their work Healey et al.[12] only proposed the SBT model but never confirmed it experimentally from the point of view of the polarizability of the oxide/electrolyte interface.

The other model postulates the existence of the hydrated layer of finite thickness within which the proton binding sites are situated. It is assumed that hydrogen ions can penetrate through the surface to the interior of this hydrated layer. The high selectivity of all these materials for hydrogen ion suggests that indeed the exchange of hydrogen ions dominates the charge-transfer process at the hydrated layer/solution interface. Clearly, in the limit of zero thickness of the hydrated layer the two theories merge. The hydration layer model allows penetration of at least one type of ion through the interface and thus considers this interface to be *nonpolarized*. How much nonpolarized depends on the value of the exchange current density of such communicating ion. The equivalent electrical model is, of course, a parallel capacitor/resistor combination. From the point of view of the ISFET it is obvious that the interface described by the capacitive model (SBT) would respond to adsorption of any charged species inside the space charge region located in the solution. On the other hand, adsorption would have little or no effect on the potential difference at the interface described by the hydration layer model because that potential difference at the nonpolarized interface is uniquely and unequivocally given by the partitioning, i.e., by the Nernst equation.

The common ground to accommodate both models has been identified by Sandifer[14] who has shown that

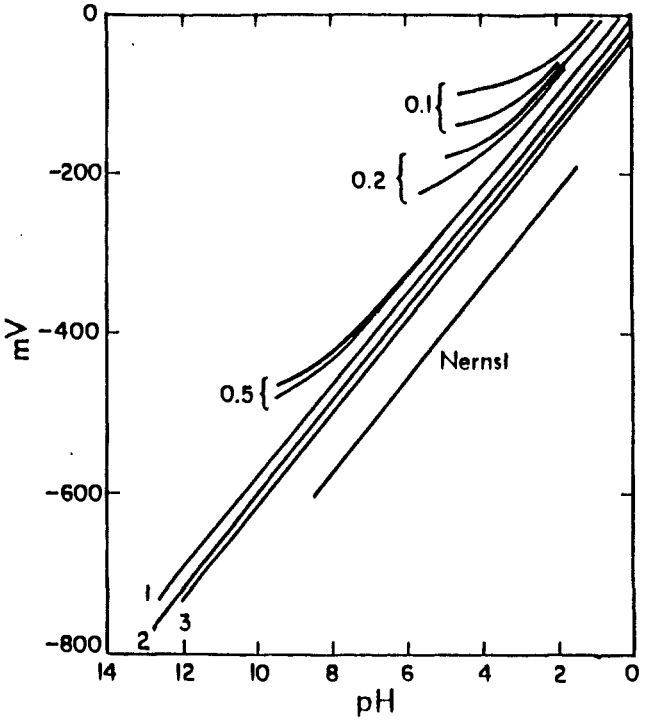

Figure 4. Dependence of the Nernst potential on the density of the binding sites (shown in molar concentration as parameter by each bracketed set) and on adsorption. Upper curves in the bracketed sets correspond to the absence of adsorption. The lower curves show the effect of 100 mM charged adsorbate (reprinted from ref 14; copyright 1988 American Chemical Society).

the sub-Nernstian response of some insulating electrode materials used in ISFETs and the presence of troublesome adsorption and stirring effects observed with poor ISE can be explained by considering the number of available binding sites and the thickness of the hydrated layer. The magnitude of the exchange current density depends on the concentration of the sites inside the hydrated layer. For a glass electrode this is estimated to be 3.2 M.[15] As the number of binding sites decreases from 3 to 0.1 M, the interfacial potential becomes increasingly affected by adsorption (Figure 4). At the same time the response deviates from theoretical the less binding sites are present. On the other hand both the adsorption effects and the sub-Nernstian behavior vanish if the thickness of the hydrated layer is allowed to increase (Figure 5). Thus, as the thickness of the hydrated layer exceeds the thickness of the space charge region, the adsorption effects and sub-Nernstian behavior disappear.

This model goes a long way toward explaining some experimental results reported in the literature for ISFETs with oxide or nitride surfaces. Unfortunately, the properties of these materials prepared in different laboratories differ substantially, which makes direct comparison of experimental results more difficult. It is known that silicon nitride forms an oxygen-rich layer at the surface whose thickness depends on the deposition conditions. This "passivation" layer seems to form rapidly but is very stable even under continuous exposure to aqueous electrolyte solutions. The hydration of this layer seems to fit the requirements and predicted behavior of the Sandifer model.

B. Micro Reference Electrode

The justification for development of potentiometric microsensors comes from their practical use: from the

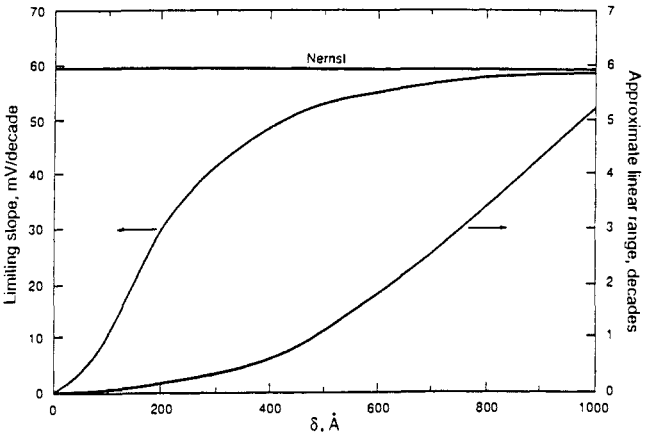

Figure 5. Dependence of the Nernst reponse on the thickness of the hydrated layer (reprinted from ref 14; copyright 1988 American Chemical Society).

saving of the sample volume and from the possibility to make a miniature multisensors. Because the well-defined reference electrode is a necessity in all potentiometric measurements, it is desirable that such an electrode has dimensions comparable to those of the active sensor. There are three basic requirements that a reference electrode must satisfy. It must be stable, reversible, and reproducible. *Stable* means that its potential will not change when the composition of the sample changes. *Reversible* means that the potential will return rapidly to its equilibrium value after a small transient perturbation. This condition implies a low charge-transfer resistance R_{ct} (high exchange current density). *Reproducibility* implies that the same electrode potential will be always obtained when the reference electrode is constructed from the same electrode/solution combinations.

The requirement of stability and reversibility (good ohmic contact) is easily satisfied by choosing an electrochemical reaction that is very fast, i.e., has a very high exchange current density ($>10^{-3}$ A cm^{-2}). An example of such an electrode reaction is the silver/silver chloride electrode, which is realized by coating a silver metal with a few microns thick silver chloride.

There have been several attempts to prepare a micro reference electrodes that would be comparable in size with the ISFET. They have followed broadly three lines of approach: Scaling down of a macroscopic reference electrode, elimination of the reference solution compartment while preserving the internal element structure (e.g., Ag/AgCl), and utilization of "inert" materials such as polyfluorinated hydrocarbons, etc., particularly in, so-called "reference FET" configuration. The last type clearly violates the requirement of the high exchange current density: There is always some potential at any interface. Unless that potential is dominated by a high exchange current density reaction, it cannot be stable. The second type, the internal element without internal compartment, violates the condition of the constant activity of the reference ion (e.g., a^{Cl}). Although such an electrode will form a good ohmic contact with the solution containing chloride ions, its potential will change with the composition of the solution. The first type, miniature conventional reference electrode, can function but only for a short period of time, depending on the actual volume of the reference solution compartment and on the conditions under which it is used. The useable lifetime is only minutes

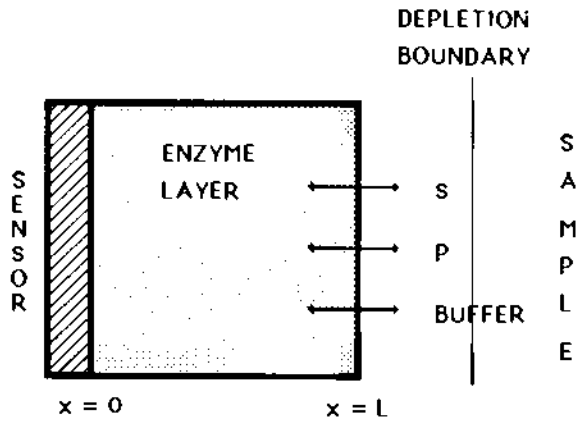

Figure 6. Schematic diagram of an enzymatic sensor (reprinted from ref 1; copyright 1989 Plenum).

to hours. The fact that such electrodes cannot sustain an outflow of the internal solution makes the liquid-junction potential unstable in practical applications. In short, there is no true "micro reference electrode" available, and in most applications a conventional macroscopic reference electrode must be used.

III. Enzyme Transistors

Enzymatic reactions combine substrate specificity with the high amplification factor. From that viewpoint they are ideal selective layers for chemical sensors.

A schematic diagram of an enzymatically coupled chemical sensor is shown in Figure 6. The geometry of the probe is chosen such that it corresponds to a semiinfinite linear diffusion; however, other, e.g., radial diffusion, geometries have been considered. The basic operating principle of an enzyme sensor is simple: An enzyme (a catalyst) is immobilized inside a layer into which the substrate(s) diffuse. Along its diffusion path, it reacts according to the Michaelis–Menten mechanism and the product(s) diffuse out of the layer into the sample solution. Any other species participating in the reaction must also diffuse in and out of the layer. Because of the combined mass transport and chemical reaction, this problem is often referred to as the *diffusion–reaction* mechanism. It is quite common in electrochemical reactions where the electroactive species, which undergo chemical transformation at the electrode, participates in some coupled chemical reactions. Mathematically, this case is described by a set of higher order partial differential equations that are usually solved numerically. Because most enzymes operate only in an aqueous environment, the immobilization matrices are usually gels, specifically hydrogels. The general diffusion–reaction equation for species i in one direction (x) is

$$\partial C_i/\partial t = +D_i(\partial^2 C_i/\partial x^2) \pm \mathcal{R}(C_i) \qquad (6)$$

When the pH-dependent Michaelis–Menten equation is substituted for the reaction term $\mathcal{R}(C_i)$, we obtain for the substrate S

$$\frac{\partial C_S}{\partial t} = D_S\frac{\partial^2 C_S}{\partial x^2} - \frac{V_m C_S}{\mathcal{R}(\mathrm{pH})(C_S + K_m)} \qquad (7)$$

It is convenient to normalize the variables in eq 7 as

$$t = \boldsymbol{t}L^2/D \qquad C_S = \boldsymbol{C}_S K_S \qquad x = \boldsymbol{x}L \qquad (8)$$

where $\boldsymbol{t}$, $\boldsymbol{C}_S$, and $\boldsymbol{x}$ are dimensionless variables and α is so-called Thiele modulus:

$$\alpha = L[V_m/K_m D_s \mathcal{R}(\mathrm{pH})]^{1/2} \qquad (9)$$

Equation 7 then becomes

$$\frac{\partial C_S}{\partial t} = D_S\frac{\partial^2 C_S}{\partial \boldsymbol{x}^2} - \frac{\alpha^2 C_S}{1 + C_S} \qquad (10)$$

For $\alpha > 10$, the mechanism is diffusion-controlled. Conversely, for small values of the Thiele modulus, the process is reaction-controlled, which means that the diffusional fluxes of all species participating in the reaction (eq 10) are greater than the reaction term. This transformation is done for all variables. This is a system of stiff, second-order partial differential equations that can be solved numerically to yield both transient and steady-state concentration profiles within the layer.[16]

The actual solution of this problem depends on the initial and boundary conditions. These, in turn, depend on the approximations chosen for the model.

As a rule, hydrogen ion is involved not only in the pH dependency of the reaction term (Thiele modulus) but also as the actively participating species involved in the acid–base equilibrium of the substrates, reaction intermediates, and products. Furthermore, enzymatic reactions are always carried out in the presence of a mobile buffer. By mobile we mean a weak acid or a weak base that can move in and out of the reaction layer, as opposed to an immobile buffer represented by the gel (and the protein) itself. Thus, we have to include the normalized diffusion–reaction equation for hydrogen ion and for the mobile buffer

$$\frac{(\partial C_{H^+})_{tot}}{\partial \boldsymbol{t}} = D_{H^+}\frac{\partial^2 C_{H^+}}{\partial \boldsymbol{x}^2} - \frac{\alpha^2 C_S}{1 + C_S} + D_{HA}\frac{\partial^2 C_{HA}}{\partial \boldsymbol{x}^2} \qquad (11)$$

where $(\boldsymbol{C}_{H^+})_{tot}/\partial \boldsymbol{t}$ is the change of the total (bound and unbound) protons within the enzyme layer and the third term is the flux of the buffer acid. For simplicity, we consider here a simple monoprotic buffer. These two equations have to be coupled with the buffer dissociation equilibrium

$$K_a = C_{H^+}C_{A^-}/C_{HA} \qquad (12)$$

Next we have to define the boundary and the initial conditions. For so-called "zero flux" sensors there is no transport of any of the participating species across the sensor/enzyme layer boundary. In that case, the first space derivatives of all variables at boundary $x = 0$ are zero:

$$\{C_S(0,t)\}'_{x=0} = \{C_{H^+}(0,t)\}'_{x=0} = \{C_{HA}(0,t)\}'_{x=0} = 0 \qquad (13)$$

In contrast, amperometric sensors would fall into the category of "non-zero-flux sensors" by this definition, and the flux of at least one of the species (product or substrate) would be given by the current through the electrode.

The lack of depletion layer at the gel/solution boundary ($x = L$) is guaranteed by stirring of the sample, which ensures that the concentrations of all species at that boundary are equal to the bulk values:

$$C_S(L,t) = C_{S,bulk} \qquad C_{HA}(L,t) = C_{HA,bulk}$$
$$C_H(L,t) = C_{H,bulk} \qquad C_A(L,t) = C_{A,bulk} \qquad (14)$$

The initial conditions are

$$C_{HA}(x,0) = C_{HA,bulk} \qquad C_A(x,0) = C_{A,bulk}$$
$$C_H(x,0) = C_{H,bulk} \qquad C_S(x,0) = 0 \text{ for } x < L \qquad (15)$$

which means that all species except the substrate are

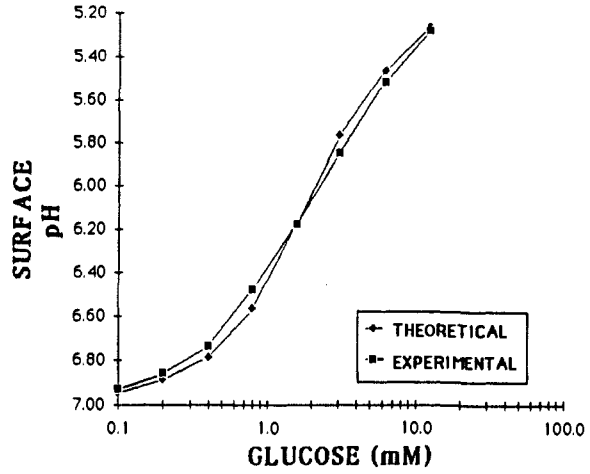

Figure 7. Calibration curve for glucose-sensitive ENFET in 0.2 mM phosphate buffer (pH 7.2) saturated with oxygen at 33 °C (reprinted from ref 16; copyright 1985 American Chemical Society).

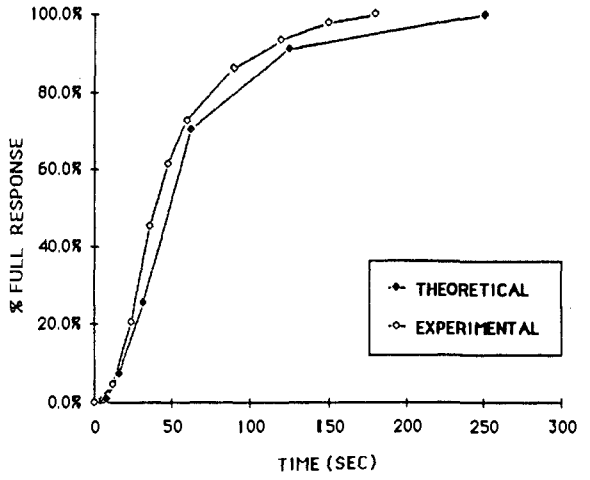

Figure 8. Time response of a glucose ENFET for concentration step from 0 to 1 mM glucose under conditions given in Figure 7 (reprinted from ref 16; copyright 1985 American Chemical Society).

initially present inside the enzyme layer.

Matching of the experimental calibration curves and of the time-response curves with the calculated ones provides the verification of the proposed model (Figures 7–9). The main goal of this excercise is determination of the optimum thickness of the enzyme layer. Because the Thiele modulus is the controlling parameter in the diffusion-reaction equation, it is obvious from eq 9 that the optimum thickness L will depend on all constants and functions included in the Thiele modulus and will vary from one kinetic scheme to another.

Other important considerations are the detection limit, dynamic range, and sensitivity. For the expected values of the diffusion coefficient (in the gel) of approximately 10^{-6} cm^2 s^{-1} and substrate molecular weights of ≈300, the detection limit is approximately 10^{-4} M. This is due to the fact that the product of the enzymatic reaction is being removed from the membrane by diffusion with approximately the same rate as it is being supplied. The dynamic range of the sensor depends on the values of K_m and V_m (which depend on the enzyme loading). Generally speaking, higher loading should extent the dynamic range at the top concentration range. It is sometimes stated incorrectly that "the enzyme sensor has close to *theoretical* dependence" or a "Nernstian response", which means that a one-

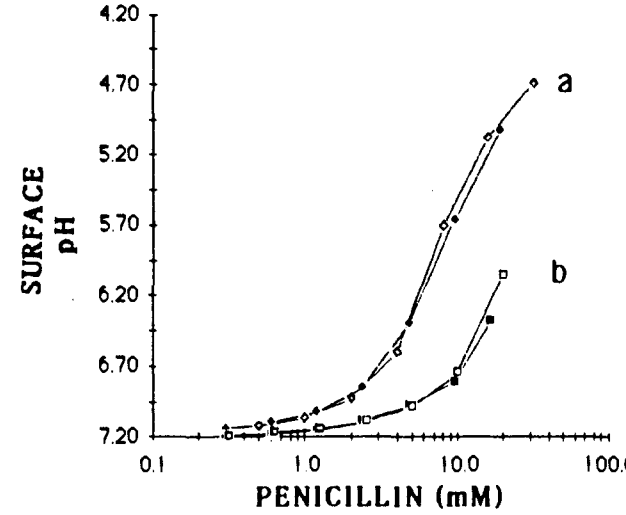

Figure 9. Calibration curve for penicillin-sensitive ENFET. Two concentrations of pH 7.2 phosphate buffer were used: (a) 20 mM and (b) 80 mM (reprinted from ref 16; copyright 1985 American Chemical Society).

decade change of *the bulk* concentration of the substrate is expected to yields a one-decade change of *the surface* ($x = 0$) concentration. It is not intuitively obvious but clearly evident from the comparison of the experimental and calculated response curves that there is no general theoretical slope, each enzymatic sensor having its own depending on the mechanism and on the conditions under which it operates. We must remember that decade/decade slope would occur only if *a constant fraction* of the product would reach the $x = 0$ interface. The upper limit of the dynamic range depends on the value of the ratio $V_m/K_m D_S \mathcal{R}$(pH) in the Thiele modulus. It can be increased by enzyme loading but, obviously, only up to a point. Normally, the dynamic range is approximately between 10^{-4} and 10^{-1} M.

The verification of the diffusion–reaction model has been done for number of enzymes and with different approximations. Mathematically, the most complex case is that of the pH-dependent, transient kinetics while the pH-independent case is considerably simpler.[17] Also, an explicit algebraic solution for a steady-state model with possible mediated transfer of protons has been found.[18] In the case of oxidation of β-D-glucose catalyzed by a glucose oxidase (GOD)/catalase system and for hydrolysis of penicillin catalyzed by β-lactamase, hydrogen ion is the species detected by the transistor surface.

It is possible to calculate and plot the concentration profiles of the participating species inside the gel layer (Figure 10). It can be seen from these plots that the concentration gradients are not linear either in the steady state or during the transition period. This shows that the assumption of a linear concentration gradient used in the early models of potentiometric enzymatic sensors is not justified. The main information that the concentration profiles provide is the value of the minimum required thickness. The thinner membranes or directly immobilized enzymes would produce a lower sensitivity. On the other hand, the thicker the enzyme layer, the slower the response. Thus, the time response can be traded for the signal to noise ratio by adjusting the thickness of the enzyme-containing layer. In some cases, a sacrifice of sensitivity may be justified for the sake of simplicity of preparation using the photolithographic process.[19]

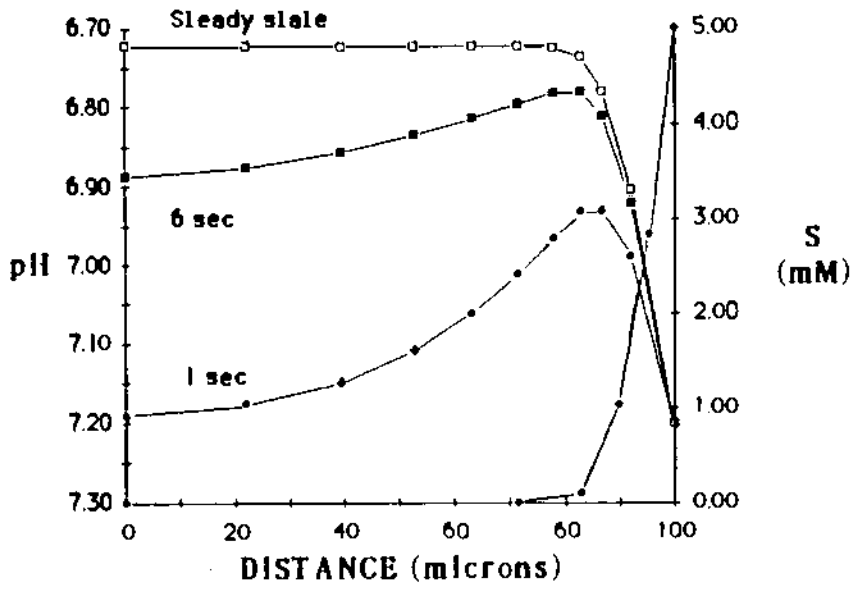

Figure 10. Concentration profile for penicillin through a 100-μm-thick membrane for concentration step from 0 to 5 mM penicillin in 2 mM pH 7.2 phosphate buffer.

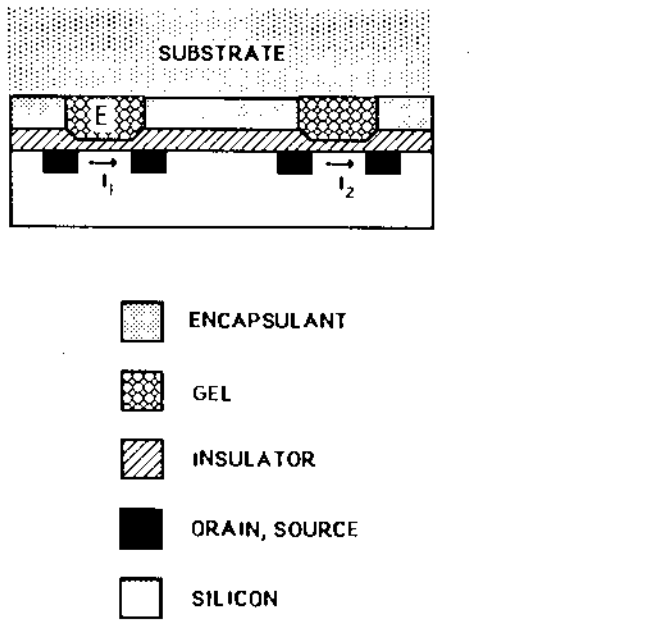

Figure 11. Diagram of a dual-gate enzymatic field effect transistor. Gate 1 contains the enzyme; gate 2 is blank.

Other parameters affecting the response characteristics of these sensors are the partitioning coefficients and the diffusion coefficients of all species and parameters related to the enzyme activity itself, such as the enzyme concentration, K_m, and V_m. They are in turn affected by the preparation of the enzyme layer, e.g., by the degree of cross-linking, by the degree of inactivation of the enzyme, etc. It is therefore not surprising to find that these devices have generally widely different lifetimes, time response, detection limits, and sensitivity. The value of the experimentally verified model is then mainly in establishing the design parameters not only for potentiometric but also for other zero-flux boundary enzymatic sensors.

Because enzymes provide such an attractive possibility for achieving chemical selectivity, enzyme electrodes were the first enzymatic chemical sensors (or first biosensors) made. The early designs used any available method of immobilization of the enzyme at the surface of the electrode. Thus, physical entrapment using dialysis membranes, meshes, and various covalent immobilization schemes has been employed. The enzyme-containing layer is simply added onto the existing ion sensor. The use of ISFETs enables precise control of the geometry of the enzyme layers as well as the miniaturization of these devices (Figure 11).

The choice of ion sensor clearly depends on the type of the enzymatic reaction, namely on the products and reagents of that reaction and on the conditions of the sample. Because each enzyme sensor has its own unique response, it is necessary to construct the calibration curve for each sensor separately. The obvious way to reduce interferences is to use two sensors in differential mode. It is possible to prepare two identical enzyme sensors and either omit or deactivate the enzyme in one of them. This sensor then acts as a reference device. If the calibration curve is constructed by plotting the difference of the two outputs as a function of concentration of the substrate, the effects of variations in the ambient composition of the sample as well as temperature and light variations can be substantially reduced.

It has been shown that the buffer capacity of the sample is the major interferant (Figure 9). This is a serious limitation particularly for practical application of these devices when the buffer capacity of the sample is not known. One possible solution to this problem, which seems to be particularly suitable for microsensors, has been recently suggested.[20] It is possible to incorporate an inert electrode *inside the gel layer* and use it as a proton generator in order to keep the pH inside the layer constant. The faradaic current, which depends on the rate of production of protons by the enzymatic reaction, then becomes the output, which can be related to the concentration of the substrate in the solution. The initial experiments have shown that this approach is feasible. The main problem is, however, the constancy of the *current efficiency* of the proton-generating current.

IV. Gas Sensors

The osmotic equilibrium involving the internal solution, which is not a serious problem in macroscopic Severinghaus electrodes, becomes a serious limitation in potentiometric microsensors for the reasons discussed in section II. It is another example of direct scaling-down that does not work. There are, however, other possibilities for potentiometric sensing of gaseous molecules that are suitable for a microsensor approach. One is the chemical modulation of the electron work function,[21] discussed in the following section.

A. Work Function Sensors

Work function (WF) has not been used for the purposes of chemical sensing with the exception of hydrogen-sensitive Pd MOS transistors and capacitors. The common feature of these two structures is the metal/insulator/semiconductor capacitor. Their macroscopic equivalent is so called Kelvin probe or vibrating capacitor, which is used primarily for measurement of surface charge on insulators and of work function of solids in vacuum. It has been proposed as a gas chromatographic detector[22] in the early 1950s but was soon replaced by a simpler and more compact flame ionization detector developed at about the same time.

Electron work function is defined as the energy required to remove an electron from the bulk of a phase and place it in the vacuum reference level just outside the range of the electrostatic forces. In conductors and semiconductors it determines the operating parameters of devices using these materials. It is the most important parameter in the operation of the tunneling microscope, and it plays a major role in heterogeneous catalysis, electrocatalysis, and the kinetics of electro-

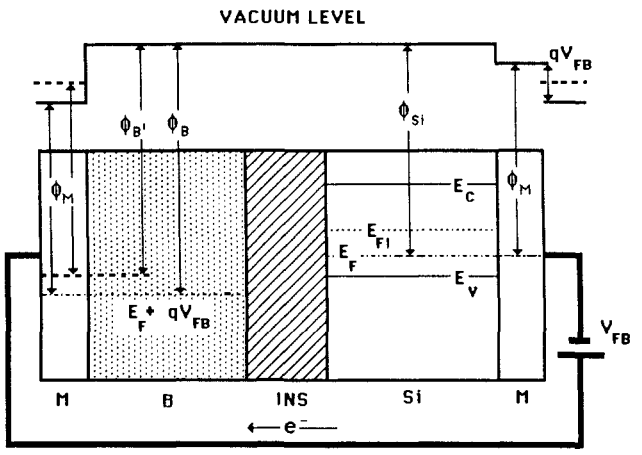

Figure 12. Effect of the work function on charge distribution in a metal–insulator–semiconductor capacitor (reprinted from ref 1; copyright 1989 Plenum).

chemical processes in general. The physical meaning of the WF, the origin of the contact potential, and the importance of the *location* of the layer to be modulated will be discussed below.

First, we have to realize that the absolute value of the electrochemical potential of a single phase (work function) cannot be measured, but the *difference* of the electrochemical potentials (difference of WF) of two phases can. The classical techniques for this measurement, besides the vibrating capacitor, are photoemission, thermionic emission, calorimetry, and semiconductor devices with metal/insulator/semiconductor capacitor.

Let us now consider the metal/selective layer/insulator/semiconductor structure shown in Figure 12. It should be noted that the surface of the selective layer B and of the metal M is clean and their work function is due only to the energy required to remove the electron from their bulk. Let us also specify that there is no electric field and therefore no space charge at the insulator/silicon interface that would result in bending of the energy bands at the insulator/semiconductor interface. In other words, the potential difference between the surface and the bulk of the semiconductor is zero ($\phi_{SB} = 0$), and the energy bands are flat. This arbitrary but convenient state is called *flatband condition.* In MIS junction the flatband condition is equivalent to the "null current" condition under which the Kelvin probe would be balanced. Throughout the ensuing manipulations, the flatband condition will be maintained with the help of an externally applied *flatband voltage* V_{FB}, if necessary. It is also assumed that no trapped charges or oriented dipoles exist inside the insulator or at its interfaces. The connecting lead is made again from the same metal M so that no additional contact potentials develop.

In order to see the effect of the chemical modulation of the work function of the selective layer B, we pass the test charge through this structure in a counterclockwise direction using the Fermi level in silicon as the starting and the final point. It is convenient to make a convention that the energy will be taken as positive when we go up and negative when we move down. We start by moving the test charge from E_F to the vacuum level above silicon, defined by ϕ_{Si}. Due to the imposed flatband condition, the vacuum level over the insulator is flat (no electric field). That defines the position of the Fermi level inside the selective layer, which is ϕ_B below the vacuum level. Because there is an ohmic contact (exchange of electrons) between M and B, the Fermi level inside B is the same as in B and defines the position of the vacuum level for M (ϕ_M above the Fermi level). The metal M on the left-hand side of Figure 12 is the same as on the right-hand side and so is its vacuum level. Because the Fermi level in M and in Si are equal, there is again a contact potential at that interface. Now we see that the Fermi levels in the same metal M are *not equal.* The resulting potential difference is the flatband voltage V_{FB}, which must be externally applied in order to satisfy the flatband condition. When we add up the energy contributions beginning and ending at the silicon Fermi level, the total energy must be zero

$$\phi_{Si} - \phi_B + \phi_M + qV_{FB} + (\phi_{Si} - \phi_M) - \phi_{Si} = 0 \qquad (16)$$

or

$$qV_{FB} = \phi_B - \phi_{Si} \qquad (17)$$

Thus, the flatband voltage (multiplied by the test charge) equals the difference in the electron work function of the selective layer B and of the semiconductor Si. If there are other charges or dipoles in this structure of whatever origin (nonideal junctions), they must be added to the V_{FB}.

There is a different way to look at the origin of the flatband voltage. Because the electron work function of layer B is larger (e.g., longer arrow) than that of the silicon, it can be argued that electrons are bound more tightly in that layer. When the M/B/INS/Si structure is assembled, electrons flow from Si to B. Thus, the act of joining causes the separation of charge and the formation of the potential difference, which, without externally applied compensating voltage V_{FB}, would appear across the insulator.

Under the flatband condition different junctions will have different value of V_{FB}. When the work function of B is chemically modulated (e.g., to B'), its Fermi level is adjusted, e.g., upward as indicated by the dashed line in Figure 12. In order to satisfy the flatband condition, the V_{FB} must be reduced accordingly relative to its previous value. Such a change of the V_{FB} can be measured.

It can be shown that only the change of WF produced in the layer *adjacent to the insulator* determines the flatband voltage. This rule has one very important implication for chemical sensing. Let us suppose that a layer is prepared that is suitable for detection of some chemical species, e.g., its electron work function could be chemically modulated. If that layer is connected to the MIS structure by a wire, the WF modulation effect is canceled by the equal changes of the contact potential at the two junctions.

Thermodynamics of Chemical Modulation of WF

At equilibrium, the number of moles n of all species and their chemical (or electrochemical) potentials μ are related through the Gibbs–Duhem equation

$$\sum_i n_i \, d\mu_i = 0 \qquad (18)$$

Thus, if a new species enters the phase, according to the law of mass action, the chemical potentials of all species must change so that eq 18 remains valid. These

include the change of the electrochemical potential of electron—the Fermi level.

The electrochemical potential of an electron can be expressed as the sum of the electrostatic energy and of the chemical potential

$$\tilde{\mu} = \mu - e\phi_G \tag{19}$$

where ϕ_G is the bulk (Galvani) potential of the phase. Because this potential is referenced against vacuum level, it can be divided into the energy contributions resulting from the transfer of the electron over the outer potential Ψ and the surface (dipole) potential χ. Thus

$$\tilde{\mu} = \mu - e\chi - e\Psi \tag{20}$$

The work function of the chemically sensitive layer ϕ_L is then defined as

$$-\phi_L = \mu - e\chi \tag{21}$$

From eq 21 we see that chemical modulation of the WF can originate from two effects: action of the guest molecule on the energy state distribution in the bulk of the phase, i.e., by *absorption* term μ in eq 21, or by modulation of the surface potential, term $e\chi$ in eq 21, i.e., by *adsorption*. These two terms have different dependences on the activity of the guest molecule. The chemical potential follows the logarithmic law

$$\mu = \mu^0 + RT \ln a \tag{22}$$

whereas the surface concentration depends on the type of the adsorption isotherm, which usually has the form of a power law. In order to resolve these two types of contributions to the overall change of the work function, it is necessary to examine the modulation effect over a broad range of concentrations.[23]

In a way, the insulated gate field effect transistor with Pd gate, extensively investigated by Lundstrom,[21] is a normal field effect transistor. It can be electrically modulated as a normal IGFET, and all the equations used to describe the operation of the field effect transistor apply. Yet, it responds to the change of the partial pressure of hydrogen. This response is due to the modulation of the electron work function of the palladium gate layer as described above.

It has been shown that the mechanism of response involves a sequence of steps in which molecular hydrogen dissociates at the Pd surface and diffuses through the Pd layer as atomic hydrogen. It then accumulates at the Pd/SiO_2 interface where it gives rise to an electrical dipole. Thus, the primary source of the signal is the increase of the dipole field at this interface.

It is interesting to note that other species that can be catalytically cleaved to yield hydrogen can be also detected by the Pd IGFET. Thus, ammonia, lower hydrocarbons, and hydrogen sulfide have been found to produce a signal.[21] The general mechanism is the catalytic abstraction of hydrogen from these molecules:

$$XH_n + Pd \overset{K_{dh}}{\Rightarrow} XH_{n-1} + Pd(H) \tag{23}$$

Thus, the Pd layer serves a dual purpose: as a catalytic surface generating the interacting species and as the source of the primary signal. It has been shown that deposition of an additional layer of Al_2O_3 between Pd and SiO_2 further improves the operational characteristics of these devices, namely their drift.

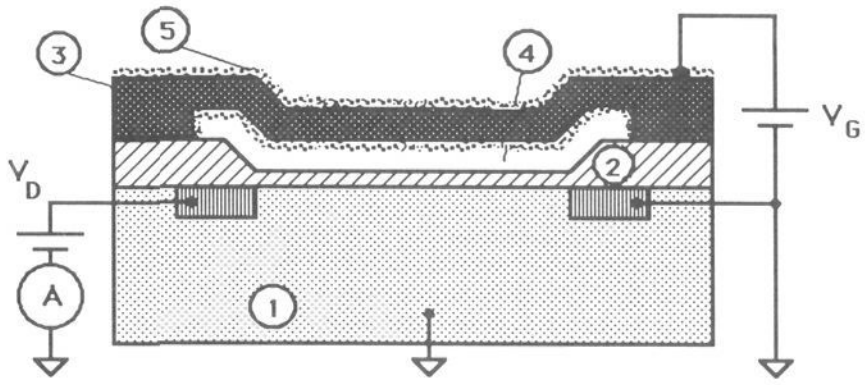

Figure 13. Schematic diagram of a suspended gate field effect transistor: 1, substrate; 2, insulator; 3, suspended metal; 4, gap; 5, selective layer (reprinted from ref 1; copyright 1989 Plenum).

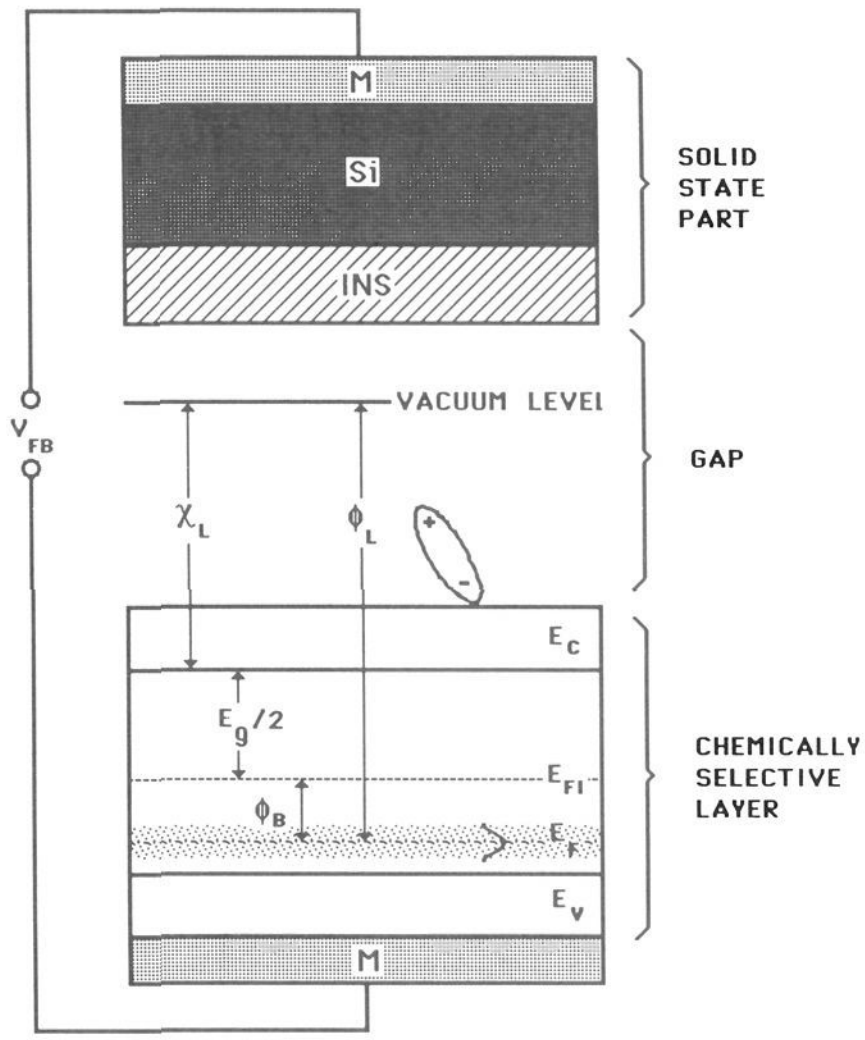

Figure 14. Energy relationships in a gap junction (reprinted from ref 1; copyright 1989 Plenum).

One drawback of a Pd IGFET is that it is restricted to sensing of hydrogen and hydrogen-producing species. A general structure allowing utilization of the chemical modulation of WF of any conducting layer is shown in Figure 13. It is called a suspended gate field effect transistor (SGFET) because the metal gate electrode, which is conventionally placed directly on top of the gate insulator, is suspended 1000–5000 Å above the solid insulator surface. This transistor is a miniature analogue of the Kelvin probe. The graphical representation of the arrangement of the gate of SGFET with an arbitrary n-type semiconducting selective layer is shown in Figure 14. The position of the energy level for the dopant, and thus the position of the Fermi level in the whole phase, depends on the intrinsic Fermi level of the pure material E_i, on the electron donor/acceptor properties of the dopant, and if the dopant is charged, on the occupational density of the states. Therefore, for a p-type material the dopant energy level (acceptor) would be positioned close to the valence band edge (E_V) and the Fermi level would be closer to that edge accordingly.

We have shown[24] that it is possible to deposit a thin (1000–3000-Å) layer of inorganic, organic, or organometallic materials underneath the suspended bridge and to study the chemical modulation of the electron WF of such layer when the device is exposed to different environments. A simple explanation of the sensing mechanism of the SGFET, which has been verified experimentally, is as follows. For a given applied gate voltage V_G, there is an equilibrium distribution of electrons between all layers including the silicon, metal bridge, and the deposited layer. When a gaseous species penetrates through the gap and into the deposited layer, it changes its affinity for electrons (one component of the WF). Thus, electrons can be either added to or withdrawn from this layer. It can be shown that the addition or withdrawal of electrons to/from the selective layer is balanced out by the electrons supplied to/from the silicon below the insulator. The transistor current then depends on the final distribution of electrons within the gate structure, i.e., on the density of electrons in the surface region of the silicon. In this respect, SGFET behaves as an ordinary MOSFET with one important exception: The gap, which is just another insulator, allows the chemical species to penetrate inside the transistor gate and interact with the electric field. If an operating value of the drain to source current is selected and maintained by means of adjusting the applied gate voltage, the amount of adjustment of V_G becomes the measured parameter equal to the change of the WF of the selective layer.

Another insulated gate FET, which operates on the principle of chemical modulation of WF, utilizes lead phthalocyanine layer as a gate. It responds to NO_2.[25]

B. High-Temperature Sensors

A potentiometric electrochemical cell consisting of a reference electrode, solid-state electrolyte(s), and an indicator electrode can provide information about the partial pressure of gas in the same way as the electrochemical cells utilizing ion-selective electrodes and liquid electrolytes do. The general mechanism is as follows: A sample gas, which is part of a *redox couple*, permeates into the solid-state structure usually through the porous electrode and sets up a reversible potential difference at the interface according to the reaction

$$\text{gas X} \pm e^- \Leftrightarrow (A)^{\pm e} \tag{24}$$

The general cell arrangement is

$$\text{Pt}\,/\,\underset{\text{species A}\pm}{\text{const act. of}}\,/\,\underset{\text{conductor}}{(A\pm)\text{ ionic}}\,/\,\underset{\text{layer AX}}{\text{gas-sensitive}}\,/\,\text{Pt,X(g)}$$

Two requirements have to be met in order to obtain a valid measurement: First, the potential difference at one interface (reference) must not be affected by changes of the composition of the sample. This is the usual requirement of a reference potential in any potentiometric measurement. Second, there must be no continuous electronic conduction through the solid electrolyte(s); otherwise, the cell would short out internally. The first requirement can be satisfied by providing a constant (reference) partial pressure of gas to one side of the otherwise symmetrical cell. This is the so-called *reference gas electrode* arrangement, which is analogous to a concentration cell. It is doubtful that such an arrangement could be miniaturized. An example of this type is the high-temperature potentiometric oxygen sensor based on yttrium-stabilized zirconia. The schematic representation of the cell is

$$O_2\text{(ref)},\ Pt/ZrO_2;\ Y_2O_3/Pt,\ O_2\text{(sample)}$$

The electrochemical reaction taking place at the two electrodes is identical:

$$\tfrac{1}{2}O_2 + e^- = \tfrac{1}{2}O_2^- \tag{25}$$

Because these measurements are done at zero net current, the oxygen ions have sufficient mobility in the solid electrolyte and the operating temperature can be lower (100–400 °C) than normally required. The cell voltage E_{cell} is related to the partial pressure of the gas by the Nernst equation for a concentration cell

$$E_{cell} = \frac{RT}{F} \ln \frac{P_{O_2}(\text{sample})}{P_{O_2}(\text{ref})} \tag{26}$$

Another possibility of realizing the constant activity of the potential-determining ion at the reference interface is to choose a solid electrolyte in such a way that the ion of the redox couple is the same as one of the major components of the electrolyte. In that case, the change of activity due to reaction with the gas can be neglected against the overall constant activity of that ion in the salt. This is the so-called *solid-state reference* arrangement. An example is the chlorine sensor in which the reference potential is set up by the constant activity of Cl^- in the solid AgCl electrolyte.

$$\begin{array}{c} \qquad\qquad\quad Cl_2 \\ Ag/AgCl/SrCl_2,\ KCl/RuO_2,\ C \\ \text{reference electrolyte indicator} \\ Ag^+\ \ Cl^- \qquad\quad Cl^-\ \ e^- \end{array}$$

The redox reaction at the indicator electrode (cathode) is

$$Cl_2 + 2e^- = Cl^- \tag{27}$$

The electrons are supplied from dissolution of the equivalent amount of silver at the anode (reference). When the chlorine partial pressure is increased in the sample, silver ions are generated at the anode and combine with the mobile chloride ions in the AgCl layer. The charge balance is maintained by transport of the chloride ions from the Sr_2Cl, KCl layer. Operation of this sensor is predicated by the low solubility of Cl_2 in the AgCl phase. It operates between 100 and 400 °C, and the dynamic range is $1–10^{-6}$ atm of P_{Cl_2}. Although it has not yet been reported, this type of sensor could be implemented in a miniature (e.g., FET) form.

High-temperature potentiometric sensors are some of the most selective sensors known.[26] It would be, therefore, particularly attractive to miniaturize them. It is possible, but the obstacle in this case is the relatively high operating temperature. The solid-state ionic materials used in these sensors are conductors at mostly higher (>400 °C) temperatures. On the other hand, it is not possible to operate solid-state devices based on silicon at temperatures above 200 °C for prolonged periods of time. Thus, a compromise operating temperature must be found. For example, the cell Sn/SnF_2/LaF_3/Pt responds to oxygen at room temperature.[27] It has not been implemented yet in a microsensor format, but it seems to be a logical thing to do. On the other hand, a typical high-temperature oxy-

gen-sensitive material, yttrium-stabilized zirconia, has been deposited on FET gate and operated as an oxygen sensor, although with some technical difficulties.[28]

V. Summary

Chemical microsensors are a growing area of analytical microinstrumentation. The miniaturization resulting from combination of traditional electrochemical and integrated circuit fabrication techniques not only has obvious practical advantages, e.g., size, sample volume speed of response, etc., but also opens some fundamentally new possibilities. Thus, the use of pH-sensitive insulators is possible only in ISFETs. The troublesome interference from buffer capacity in pH-based enzyme sensors may be mitigated by the internal generation and control of hydrogen ions inside the enzyme-containing layer. This can be conveniently done in a microfabricated enzyme electrode. Finally, a whole new class of solid-state potentiometric microsensors based on chemical modulation of the electron work function can be built around the insulated gate field effect transistor.

Glossary

a^i	ion activity
C_i	concentration of species i
C_0	gate capacitance
D	diffusion coefficient
E_{REF}	reference electrode potential
I_D	drain current
K_a	dissociation constant
K_m	Michaelis–Menten constant
L	length
q	test charge
Q_B	depletion layer charge
V_D	drain voltage
V_{FB}	flatband voltage
V_G	gate voltage
V_m	maximum reaction velocity
V_T	threshold voltage
V_T^*	ISFET threshold voltage
W	channel width
z^i	ion charge
α	Thiele modulus
χ	surface potential
ϕ_{cont}	contact potential
ϕ_F	Fermi energy (e.g., ϕ_{Si} for silicon)
ϕ_G	Galvani (electrostatic) potential of the phase
Ψ	outer potential
μ	chemical potential
$\bar{\mu}$	electrochemical potential
μ_n	electron mobility
π	interfacial potential difference
$\mathcal{R}$	reaction term

References

(1) Janata, J. *Principles of Chemical Sensors*; Plenum Press: New York, 1989.
(2) Ammann, A. *Ion-Selective Microelectrodes*; Springer-Verlag: Berlin, 1986.
(3) Morf, W. E. *Principles of Ion-Selective Electrodes and of Membrane Transport*; Elsevier: Amsterdam, 1981. Evans, A. *Potentiometry and Ion-Selective Electrodes*; Wiley: New York, 1987. Horvai, G.; Toth, K.; Pungor, E. *Anal. Chim. Acta* **1989**, *216*, 163. Solsky, R. *Anal. Chem.* **1988**, *60*, 106R.
(4) Kimura, J.; Murakami, T.; Kuriyama, T.; Karube, I. *Sens. Actuators* **1988**, *15*, 435.
(5) Shoji, S.; Esashi, M.; Matsuo, T. *Sens. Actuators* **1988**, *14*, 101.
(6) Van der Vlekkert, H.; Francis, C.; Grisel, A.; DeRooij, N. *Analyst* **1988**, *113*, 1029.
(7) Harrison, J. D.; Cunningham, L. L.; Li Xizhong; Teclemariam, A.; Permann, D. *J. Electrochem. Soc.* **1988**, *135*, 2473.
(8) Fogt, E. J.; Untereker, D. F.; Norenberg, M. S.; Meyerhoff, M. E. *Anal. Chem.* **1985**, *57*, 1995.
(9) Li Xizhong; Veerporte, M. J.; Harrison, J. D. *Anal. Chem.* **1988**, *60*, 493.
(10) Bergveld, P. *IEEE Trans. Biomed. Eng.* **1970**, *BME-19*, 70.
(11) Matsuo, T.; Esashi, M.; Inuma, K. *Dig. Joint Meet. Tohoku Sect. IEEEJ* **1971**.
(12) Yates, D. E.; Levine, S.; Healey, T. W. *J. Chem. Soc., Faraday Trans. 1* **1974**, *70*, 1807. Yates, D. E.; Healey, T. W. *J. Colloid Interface Sci.* **1976**, *55*, 9.
(13) Bousse, L.; Bergveld, P. *Sens. Actuators* **1984**, *6*, 65.
(14) Sandifer, J. R. *Anal. Chem.* **1988**, *69*, 1553.
(15) Eisenman, G. *Glass Electrodes for Hydrogen and Other Cations*; Dekker: New York, 1969; Chapter 7.
(16) Caras, S. D.; Janata, J.; Saupe, D.; Schmidt, K. *Anal. Chem.* **1985**, *57*, 1917. Caras, S. D.; Petelenz, D.; Janata, J. *Anal. Chem.* **1985**, *57*, 1920. Caras, S. D.; Janata, J. *Anal. Chem.* **1985**, *57*, 1924.
(17) Edowes, M. J. *Sens. Actuators* **1985**, *7*, 97.
(18) Varanasi, S.; Ogundiran, S. O.; Ruckenstein, E. *Biosensors* **1988**, *3*, 269.
(19) Kumira, I.; Saito, A.; Ito, N.; Nakamoto, S.; Kuriyama, T. *J. Membr. Sci.* **1989**, *291*, 3. Hanazato, Y.; Inatomi, K.; Nakako, M.; Shiono, S.; Maeda, M. *Anal. Chim. Acta* **1988**, *212*, 49. Fu, H.; Anzai, J.; Osa, T.; Matsuo, T. *Chem. Pharm. Bull.* **1988**, *36*, 1190. Tamiya, E.; Karube, I.; Kitagawa, Y.; Ameyama, M.; Nakashima, K. *Anal. Chim. Acta* **1988**, *207*, 77.
(20) Van der Schoot, B. H.; Bergveld, P. *Anal. Chim. Acta* **1987**, *199*, 157.
(21) Lundstrom, I.; Svensson, C. In *Solid State Chemical Sensors*; Janata, J., Huber, R. J., Eds.; Academic Press: New York, 1985.
(22) Phillips, C. S. G. *J. Sci. Instrum.* **1951**, *28*, 342.
(23) Cassidy, J.; Pons, B. S.; Janata, J. *Anal. Chem.* **1986**, *58*, 1757.
(24) Josowicz, M.; Janata, J. In *Chemical Sensor Technology*; Seiyama, T., Ed.; Elsevier: New York, 1988; Vol. 1.
(25) Burr, P. M.; Jefferey, P. D.; Benjamin, J. D.; Uren, M. J. *Thin Solid Films* **1987**, *151*, L111.
(26) Worrel, W. L. *Solid State Ionics* **1988**, *28–30*, 1215.
(27) Miura, N.; Hisamoto, J.; Yamazoe, N.; Kuwata, S. *Appl. Surf. Sci.* **1987**, *33–34*, 1253.
(28) Miyahara, Y.; Tsukada, K.; Miyagi, H. *J. Appl. Phys.* **1988**, *63*, 2431.